JACS
JOURNAL OF THE AMERICAN CHEMICAL SOCIETY
Communication
pubs.acs.org/JACS

Single Particle Detection by Area Amplification: Single Wall Carbon Nanotube Attachment to a Nanoelectrode

Jun Hui Park,[‡] Scott N. Thorgaard,[†] Bo Zhang, and Allen J. Bard*

Center for Electrochemistry, Department of Chemistry and Biochemistry, The University of Texas at Austin, Austin, Texas 78712, United States

Supporting Information

ABSTRACT: We describe the electrochemical detection of single nanoparticle (NP) attachment on a nanoelectrode by the increase in the active electrode area. The attachment of gold NP-decorated single wall carbon nanotubes (Au-SWCNTs) was observed by their current−time transients for ferrocenemethanol (FcMeOH) oxidation. Since the attached Au-SWCNT increases the electroactive area available for FcMeOH oxidation, the current increases after attachment of the particle. The "staircase" shape of the current response establishes that the particles do not become deactivated for the outer-sphere electron transfer reaction after attachment. Au-SWCNTs migrate to and are held at the nanoelectrode by an electric field. However, SWCNTs that are not decorated with a gold NP produce only a sharp transient ("blip") response.

We describe here a new method of examining interactions of single NPs with an electrode that was applied to collisions of single wall carbon nanotubes (SWCNTs) with a nanometer-sized ultramicroelectrode (UME). The method is based on recognizing the increase in electrode area upon collision and adhesion of a conductive NP. Our previous studies showed the detection of single-NP collision events at a UME by catalytic current amplification.[1−6] This catalytic current amplification method was essential for detecting NPs at a micrometer-scale electrode. However, in this approach, deactivation of the NP for the electrocatalytic reaction (e.g., by adsorption of impurities) can cause a decay in the current, and this effect makes it more difficult to model the NP current after the collision. Studies with electrode reactions that do not involve electrocatalysis (e.g., simple outer-sphere electron transfers, as described here) suffer less from these deactivation effects, as will be shown.

An alternative approach for studying collisions involves metal NPs that can be oxidized (and decomposed) upon collision.[7] In this case, the NPs maintain contact with an electrode surface for only a short time following the collision and show a transient response. Here we report monitoring of NP attachment at a nanoelectrode carrying out ferrocenemethanol (FcMeOH) oxidation, a simple outer-sphere electron-transfer reaction[8] in which neither the reactant nor the product strongly interact with the electrode surface. A stepwise current increase was obtained after each single particle attachment; this current increase was caused by a change in the active area for FcMeOH oxidation. In this case, there was no observed decrease in the steady-state current following the collision, suggesting no deactivation of the NP surface by impurity adsorption or bubble formation.

To detect NP attachment by an increase in electrode area, the size of the particle and the size of the electrode should be comparable, so the observed current change is readily detectable. The NP sticks to the surface of the nanometer-sized UME and maintains contact, implying electron tunneling from the UME to the contacting NP. When the size of the particle is much smaller than the size of electrode, the current increment after attachment of the particle is negligible. Therefore, nanometer-sized NPs cannot be detected in this way at micrometer-sized UMEs. Conversely, when the size of the particle is much larger than the size of electrode, the collision frequency is extremely low because of the small NP diffusion coefficient.[9] Moreover, large metal NPs (>300 nm) quickly settle out of the solution because of their mass.[10]

At the nanoelectrode, the diffusional collision flux (f_{diff}) decreases as the size of the electrode decreases (eq 1):

$$f_{diff} = 4D_pC_pr \quad (1)$$

where D_p is the diffusion coefficient of the NP, C_p is the NP concentration, and r is the radius of the nanoelectrode. An additional driving force (e.g., due to convection or migration) would increase the collision frequency and enable the detection of single NPs at the nanoelectrode at smaller C_p. In this study, we used an electric field (migration) to attract the NPs to the nanoelectrode.[11] However, at a nanosized electrode, only a small electric field is generated because of the small faradaic current flow,[12] so the mobility of the NPs was enhanced by increasing the charge on each NP. This can be accomplished by adsorption of highly charged surfactants [e.g., DNA, poly(ethylene glycol)],[13] but a long surfactant backbone can hinder electron transfer between the NP and the nanoelectrode.[6] Therefore, usable surfactants were limited to small molecules (e.g., citrate) that allow tunneling to the electrode. Here, water-dispersed SWCNTs capped with sodium dodecyl sulfate were used to modify Au NPs.[14] SWCNTs can migrate easily in an electric field because of their high charge and low density. Moreover, a SWCNT can contribute to electron transfer, and a multiwall carbon nanotube with a higher conductivity due to the greater thickness of the annular cross section might also be used.[15]

Received: January 16, 2013
Published: March 26, 2013

   dx.doi.org/10.1021/ja4000917 | J. Am. Chem. Soc. 2013, 135, 5258−5261

SWCNTs modified with Au NPs (designated as Au-SWCNTs) were obtained by SWCNT-templated growth of Au NPs.[16] From boiling-water-dispersed SWCNTs in the presence of $AuCl_4^-$ and citrate, SWCNTs tethered to ~20 nm diameter Au NPs were obtained (Figure 1). Au-SWCNTs with

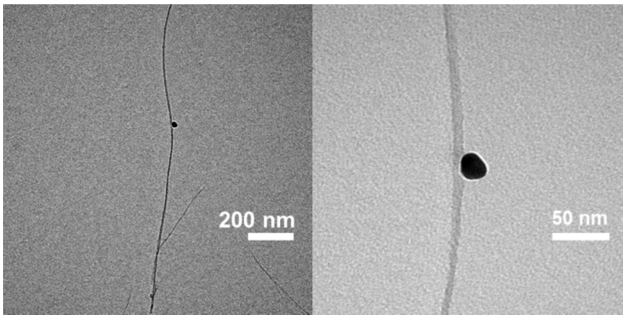

Figure 1. TEM images of an individual Au-SWCNT.

more than one tethered Au NP settled out quickly because of their greater mass, so employing only the supernatant ensured that well-dispersed Au-SWCNTs having only one or zero tethered Au NPs, as observed by TEM, were used for electrochemical detection.

As suggested in Scheme 1, Au-SWCNTs migrate to a Pt nanoelectrode because oxidation of FcMeOH to positively

Scheme 1. Pictorial Representation of the Attachment of a CNT-Modified Au NP at a Pt Nanoelectrode

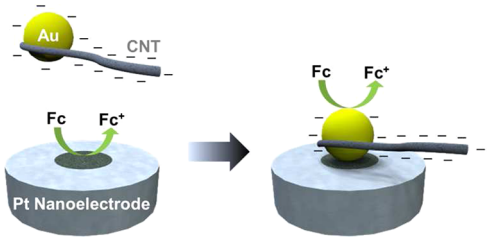

charged ferrocenium methanol creates a charge imbalance (electric field) near the nanoelectrode that attracts negatively-charged particles. By increasing the FcMeOH concentration to saturation, we obtained a larger current and charge imbalance near the nanoelectrode. We also used a low concentration of supporting electrolyte (100 μM KNO_3) to avoid decreasing the transference number of the NP. The attraction of the negatively charged Au-SWCNT toward the nanoelectrode by the electric field thus increased its mass-transfer rate and also may have played a role in its adhesion to the electrode due to the high metal–SWCNT binding energy.[17,18] Oxidation of FcMeOH probably occurs via direct electron transfer from the Au-SWCNT to the nanoelectrode. Under these conditions, Au-SWCNTs that collided and attached to the UME resulted in an instantaneous current increase to a steady-state current that remained constant for over 250 s, as shown in Figure 2. This was difficult to accomplish in electrocatalytic-based studies[1−3] and is consistent with the fact that outer-sphere electron-transfer reactions are less affected by impurity adsorption than inner-sphere reactions.

We can estimate the Au-SWCNT size from the current increment and determine the electrode dimensional change by this approach. Figure 3 shows a dimensionless plot of the simulated current change based on the assumption that the Au-

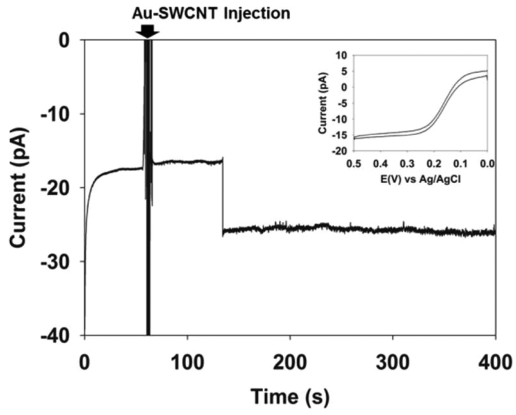

Figure 2. Chronoamperometric curve for attachment of a single Au-SWCNT at the Pt nanoelectrode (~30 nm diameter) in the presence of 4 mM FcMeOH, 100 μM KNO_3, and 85 ng/mL Au-SWCNTs. The inset shows the cyclic voltammogram for the Pt nanoelectrode. The data acquisition time was 50 ms, and the applied potential was +0.4 V vs Ag/AgCl. The large noise upon injection of the NPs was caused by opening of the Faraday cage.

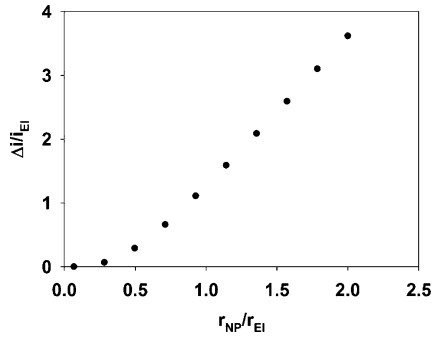

Figure 3. Simulated results for the relative magnitude of the electrode current increase ($\Delta i/i_{El}$) after NP attachment as a function of the relative size of the NP (r_{NP}/r_{El}), where r_{NP} and r_{El} are the radii of a spherical NP and a disk electrode, respectively. The NPs are assumed to be ideally spherical.

SWCNT lands at the center of the disk electrode [see the Supporting Information (SI)]. This dimensionless plot is valid at least for nano- to micrometer-sized electrodes. The relative size of the current step ($\Delta i/i_{El}$), where i_{El} is the current for the nanoelectrode, is linearly related to the relative size of the NP (r_{NP}/r_{El}) when the NP is larger than the electrode ($r_{NP}/r_{El} > 1$). When the NP is far smaller than the electrode (i.e., for $r_{NP}/r_{El} < 0.1$), the total current is barely affected by attachment of the NP. The current increment can also vary with the landing position on the UME. For example, when the comparatively small NP lands on the edge of the disk electrode, the current increment is larger than when it lands in the center because the disk electrode has a higher flux (current density) at the edge.[11,12] It was difficult to calculate the expected area of the Au-SWCNT because the geometry of the SWCNT was not clear and there was a distribution of sizes and chirality. On the basis of the observed current increment in Figure 2, the attached Au-SWCNT was roughly equivalent to a sphere with a diameter of ~19 nm.

We tried to observe the capture of non-SWCNT-tethered citrate-capped Au and Pt NPs of different sizes (from 4 to 50 nm diameter) at a 15 nm nanoelectrode but did not detect any collisions (Figure 4, red line). The SWCNT adds some area

dx.doi.org/10.1021/ja4000917 | J. Am. Chem. Soc. 2013, 135, 5258−5261

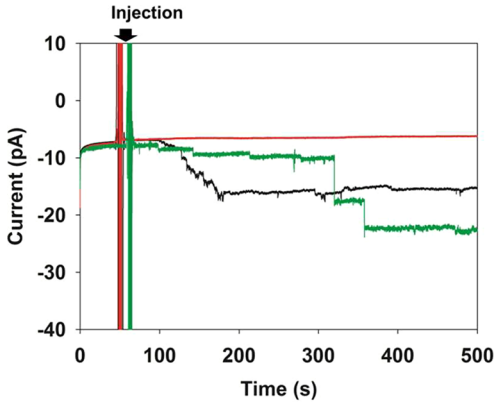

Figure 4. Chronoamperometric curves after injection of ~9 nm diameter Au NPs (red line, 40 pM), SWCNTs (black line, 180 ng/mL), and Au-SWCNT (green line, 85 ng/mL) into the electrolyte solution containing 4 mM FcMeOH and 100 μM KNO_3. A Pt nanoelectrode with a diameter of ~15 nm was used. The sample time was 50 ms, and the applied potential was +0.4 V vs Ag/AgCl.

and also promotes migration of the Au NP by providing a larger charge, as the smaller electric charge on the NPs alone is insufficient to attract and hold the citrate-capped metal NPs by themselves. Even with a higher concentration of citrate-capped metal NPs (e.g., ~100 pM), at which a diffusional collision event at a nanometer-sized UME should be observed according to eq 1, no collision response was seen over 1000 s, which implies an inability to establish a good contact between the NP and the nanometer-sized UME. However, it was possible to detect SWCNTs alone at nano- to micrometer-sized UMEs; these produced a noisy current with a sharp transient (blip) response (Figure 4, black line). This noisy current response may be understood as migration and contact of SWCNTs to the electrode. This was verified by changing the concentration of supporting electrolyte in the cell, as shown in Figure 5. Upon

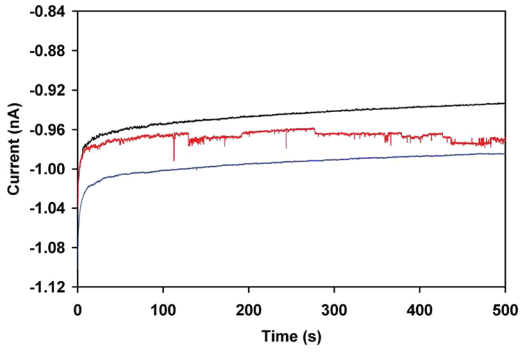

Figure 5. Chronoamperograms recorded for a 2 μm diameter Pt UME in 2.5 mM FcMeOH with 1 mM KCl (black line) and following the successive additions of first 300 ng/mL SWCNTs (red line) and second 100 mM KCl (blue line) to the same cell. Additions were performed at open circuit without removing the UME from the electrolyte solution. The applied potential was +0.5 V vs Ag/AgC, and the sample time was 100 ms.

addition of SWCNTs to a cell containing 1 mM supporting electrolyte, a similar spiky current response was observed at a 2 μm diameter Pt UME (Figure 5, red line). When the supporting electrolyte concentration in the same cell was increased to 100 mM, the spiky response disappeared (Figure 5, blue line) because of decreased migration of the SWCNTs. The persistent overall increase in the electrode current here reflects earlier buildup of SWCNTs at the UME surface.

The different electronic properties of SWCNTs may explain the variable current response for SWNTs alone, as the resistance of CNTs increases by an order of magnitude depending on the NT structure and conjugation of the surfactant.[15,19] Stacking of CNTs at the nanoelectrode would also result in an increase in current due to electroactivity of the CNT surface. For the present observations of SWCNTs, the current increased with a few small current steps (1−2 pA) and many irregular, spiked features. The current step size upon Au-SWCNT attachment suggests that the SWCNT can account for 10−20% of the total current. Varying the concentration of SWCNTs and studying them with a 2 μm Pt UME offered additional insight into their variable current response. As shown in Figure S1 in the SI, the frequency of spiked and steplike features increased with increasing SWCNT concentration as a result of a higher rate of SWCNT collisions (see the SI). The short-lived spiked features and decreasing current steps may indicate variable or intermittent contact between single SWCNTs and the UME surface. In contrast to experiments with SWCNTs alone, upon the introduction of Au-SWCNTs to the nanoelectrode cell, large and clear current steps (6−9 pA) without deactivation were observed (green line in Figure 4). These larger, more stable steps indicate that the Au NP contacts and sticks to the nanoelectrode and provides a stable surface for FcMeOH oxidation. An alternative explanation, suggested by a reviewer, is that the nanoelectrode may be slightly recessed within the glass sheath, so that the Au-SWCNT cannot make direct contact with it but is held on the surrounding insulator in a way that open-circuit (substrate) positive feedback can occur. Such positive-feedback current has been found with an immobilized SWCNT in scanning electrochemical microscopy.[20]

To provide evidence that the Au-SWCNTs are directly attached to the electrode, a carbon-fiber UME (10 μm diameter) was used to accumulate Au-SWCNTs; the results are shown in Figure 6. After accumulation of Au-SWCNTs at

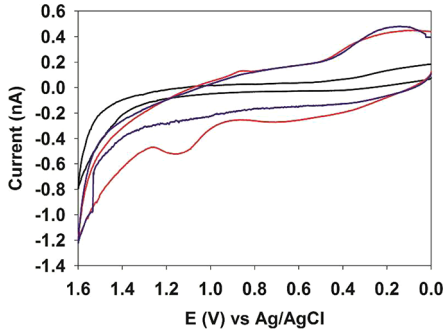

Figure 6. Cyclic voltammograms for Au-SWCNTs accumulated on a carbon UME (red line), showing characteristic Au surface waves; SWCNTs on a carbon UME (blue line); and a bare carbon UME (black line) immersed in 0.1 M H_2SO_4. The diameter of the carbon UME was 10 μm.

the carbon UME for 350 s at a potential of 0.4 V in the electrolyte solution, the carbon UME with Au-SWCNTs attached was removed, gently washed with water, and then transferred into a 0.1 M H_2SO_4 solution. Cyclic voltammograms showed the characteristic Au oxidation peak at ~1.15 V vs Ag/AgCl and Au oxide reduction peak at ~0.85 V vs Ag/

dx.doi.org/10.1021/ja4000917 | J. Am. Chem. Soc. 2013, 135, 5258−5261

AgCl, as in previous reports.[21] The redox peaks for Au oxide gradually diminished after repeated redox cycling. Neither a CNT-modified carbon UME nor a bare carbon UME showed these peaks, although the CNT-modified carbon UME showed increased capacitance relative to the bare electrode because of an increased electroactive area.

We have established that the attachment of single NPs to nanometer-sized UMEs can be detected by an increase in the electrode area. This general approach offers a simple and straightforward method of identifying a single-NP collision event and complements the approach where insulating single-NP events cause a current decrease. The results highlight the effectiveness of migration as a means of moving and capturing single NPs at a UME. This experimental approach suggests a way to capture a single NP and investigate its characteristics, in particular its size, shape, and surface-dependent electrocatalytic properties.

NPs have been widely studied for catalytic applications because of their unique physical and chemical properties, which depend on their size and structure.[22−24] Extensive studies have provided ensemble-averaged data on NPs. However, the catalytic properties of well-characterized single NPs have yet to be reported.[21,25] In view of the recent interest in electrochemical studies at the single-NP level,[26,27] there is value in techniques that allow the capture of single NPs from solution. Finally, this method might also be applicable to the study of the behavior of single biomolecules (e.g., enzymes) using sufficiently small electrodes.[28]

■ ASSOCIATED CONTENT

Supporting Information

Experimental and simulation details. This material is available free of charge via the Internet at http://pubs.acs.org.

■ AUTHOR INFORMATION

Corresponding Author

ajbard@mail.utexas.edu

Present Addresses

‡J.H.P.: Department of Chemistry Education, Chonbuk National University, 567 Baekje-daero, Jeonju-si, Jeollabuk-do 561-756, Korea.

†S.N.T.: Winona State University, Pasteur Hall 320, Winona, MN 55987.

Notes

The authors declare no competing financial interest.

■ ACKNOWLEDGMENTS

We appreciate helpful comments by the reviewers and support from the Robert A. Welch Foundation (F-0021) and the National Science Foundation (CHE-1111518) for the experimental studies. The nanometer-sized electrode preparation work was supported by the Department of Defense, Defense Threat Reduction Agency (Contract HDTRA1-11-1-0005).

■ REFERENCES

(1) Xiao, X.; Bard, A. J. *J. Am. Chem. Soc.* **2007**, *129*, 9610.

(2) Xiao, X.; Fan, F.-R. F.; Zhou, J.; Bard, A. J. *J. Am. Chem. Soc.* **2008**, *130*, 16669.

(3) Kwon, S. J.; Fan, F.-R. F.; Bard, A. J. *J. Am. Chem. Soc.* **2010**, *132*, 13165.

(4) Zhou, H.; Fan, F.-R. F.; Bard, A. J. *J. Phys. Chem. Lett.* **2010**, *1*, 2671.

(5) Bard, A. J.; Zhou, H.; Kwon, S. J. *Isr. J. Chem.* **2010**, *50*, 267.

(6) Xiao, X.; Pan, S.; Jang, J. S.; Fan, F.-R. F.; Bard, A. J. *J. Phys. Chem. C* **2009**, *113*, 14978.

(7) Kahk, J. M.; Rees, N. V.; Pillay, J.; Tshikhudo, R.; Vilakazi, S.; Compton, R. G. *Nano Today* **2012**, *7*, 174.

(8) Bard, A. J.; Faulkner, L. R. *Electrochemical Methods: Fundamentals and Applications*, 2nd ed.; Wiley: New York, 2001; Chapter 3, pp 115−117.

(9) Einstein, A. *Ann. Phys.* **1905**, *17*, 549.

(10) Ziegler, C.; Eychmüller, A. J. *J. Phys. Chem. C* **2011**, *115*, 4502.

(11) Quinn, B. M.; van't Hof, P. G.; Lemay, S. G. *J. Am. Chem. Soc.* **2004**, *126*, 8360.

(12) Park, J. H.; Boika, A.; Park, H. S.; Lee, H. C.; Bard, A. J. *J. Phys. Chem. C* **2013**, DOI: 10.1021/jp3126494.

(13) Ackerson, C. J.; Sykes, M. T.; Kornberg, R. D. *Proc. Natl. Acad. Sci. U.S.A.* **2005**, *102*, 13383.

(14) O'Connell, M. J.; Bachilo, S. M.; Huffman, C. B.; Moore, V. C.; Strano, M. S.; Haroz, E. H.; Rialon, K. L.; Boul, P. J.; Noon, W. H.; Kittrell, C.; Ma, J.; Hauge, R. H.; Weisman, R. B.; Smalley, R. E. *Science* **2002**, *297*, 593.

(15) Dai, H.; Wong, E. W.; Lieber, C. M. *Science* **1996**, *272*, 523.

(16) Choi, H. C.; Shim, M.; Bangsaruntip, S.; Dai, H. *J. Am. Chem. Soc.* **2002**, *124*, 9058.

(17) Durgun, E.; Dag, S.; Ciraci, S.; Gülseren, O. *J. Phys. Chem. B* **2004**, *108*, 575.

(18) Maiti, A.; Ricca, A. *Chem. Phys. Lett.* **2004**, *395*, 7.

(19) Geng, H.-Z.; Kim, K. K.; So, K. P.; Lee, Y. S.; Chang, Y.; Lee, Y. H. *J. Am. Chem. Soc.* **2007**, *129*, 7758.

(20) Kim, J.; Xiong, H.; Hofmann, M.; Kong, J.; Amemiya, S. *Anal. Chem.* **2010**, *82*, 1605.

(21) Li, Y.; Cox, J. T.; Zhang, B. *J. Am. Chem. Soc.* **2010**, *132*, 3047.

(22) Arenz, M.; Mayrhofer, K. J. J.; Stamenkovic, V.; Blizanac, B. B.; Tomoyuki, T.; Ross, P. N.; Markovic, N. M. *J. Am. Chem. Soc.* **2005**, *127*, 6819.

(23) Narayanan, R.; El-Sayed, M. A. *Nano Lett.* **2004**, *4*, 1343.

(24) Hvolbæk, B.; Janssens, T. V. W.; Clausen, B. S.; Falsig, H.; Christensen, C. H.; Nørskov, J. K. *Nano Today* **2007**, *2*, 14.

(25) Chen, P.; Xu, W.; Zhou, X.; Panda, D.; Kalininskiy, A. *Chem. Phys. Lett.* **2009**, *470*, 151.

(26) Shan, X.; Díez-Pérez, I.; Wang, L.; Wiktor, P.; Gu, Y.; Zhang, L.; Wang, W.; Lu, J.; Wang, S.; Gong, Q.; Li, J.; Tao, N. *Nat. Nanotechnol.* **2012**, *7*, 668.

(27) Cox, J. T.; Zhang, B. *Annu. Rev. Anal. Chem.* **2012**, *5*, 253.

(28) Bard, A. J. *ACS Nano* **2008**, *2*, 2437.